New Approaches in Modeling and Simulation of CO2 Absorption Reactor by Activated Potassium Carbonate Solution

Authors:

Maria Harja, Gabriela Ciobanu, Tatjána Juzsakova, Igor Cretescu

Date Submitted: 2019-05-16

Keywords: activated carbonate–bicarbonate solution, gas purification, reactor modeling, CO2 absorption

Abstract:

The increase of CO? concentration in the atmosphere is in strong relation with the human-induced warming up due to industrial processes, transportation, etc. In order to reduce the CO? content, end of pipe post-combustion methods can be used in addition to other methods and techniques. The CO? capture by absorption in potassium carbonate?bicarbonate activated solutions remains a viable method. In this study, a mathematical model for a packed bed reactor has been developed and tested. The mathematical model is tested for an industrial reactor based on CO? absorption in Carsol solutions. The proposed model was validated by resolving for CO? and water content, carbonate?bicarbonate, concentrations etc. For each operational parameter the error was calculated. The error for CO? concentration is up to 4%. The height of the packed reactor is calculated as function of CO? concentration in the final gas phase. The validated model can also be used for absorbing other CO? streams taking into account the fact that its efficiency was proved in industrial scale. Future reactors used for CO? absorption should consist of two parts in order to use partially regenerated solutions in the first part, with significant energy savings in the operational costs.

Record Type: Published Article

Submitted To: LAPSE (Living Archive for Process Systems Engineering)

Citation (overall record, always the latest version): LAPSE:2019.0566
Citation (this specific file, latest version): LAPSE:2019.0566-1
Citation (this specific file, this version): LAPSE:2019.0566-1v1

DOI of Published Version: https://doi.org/10.3390/pr7020078

processes

MDPI

Article

New Approaches in Modeling and Simulation of CO_2 Absorption Reactor by Activated Potassium Carbonate Solution

Maria Harja [1], Gabriela Ciobanu [1], Tatjána Juzsakova [2] and Igor Cretescu [3,*]

[1] Departments of Chemical Engineering, Faculty of Chemical Engineering and Environmental Protection, "Gheorghe Asachi" Technical University of Iasi, Prof. dr. doc. D. Mangeron Street no. 73, 700050 Iasi, Romania; mharja@tuiasi.ro (M.H.); gciobanu@tuiasi.ro (G.C.)

[2] Institute of Environmental Engineering, University of Pannonia, Egyetem St. 10, HU-8200 Veszprém, Hungary; yuzhakova@almos.uni-pannon.hu

[3] Department of Environmental Engineering, Faculty of Chemical Engineering and Environmental Protection, "Gheorghe Asachi" Technical University of Iasi, Prof. dr. doc. D. Mangeron Street no. 73, 700050 Iasi, Romania

* Correspondence: icre@ch.tuiasi.ro; Tel.: +40-741914342

Received: 29 December 2018; Accepted: 28 January 2019; Published: 4 February 2019

Abstract: The increase of CO_2 concentration in the atmosphere is in strong relation with the human-induced warming up due to industrial processes, transportation, etc. In order to reduce the CO_2 content, end of pipe post-combustion methods can be used in addition to other methods and techniques. The CO_2 capture by absorption in potassium carbonate–bicarbonate activated solutions remains a viable method. In this study, a mathematical model for a packed bed reactor has been developed and tested. The mathematical model is tested for an industrial reactor based on CO_2 absorption in Carsol solutions. The proposed model was validated by resolving for CO_2 and water content, carbonate–bicarbonate, concentrations etc. For each operational parameter the error was calculated. The error for CO_2 concentration is up to 4%. The height of the packed reactor is calculated as function of CO_2 concentration in the final gas phase. The validated model can also be used for absorbing other CO_2 streams taking into account the fact that its efficiency was proved in industrial scale. Future reactors used for CO_2 absorption should consist of two parts in order to use partially regenerated solutions in the first part, with significant energy savings in the operational costs.

Keywords: CO_2 absorption; reactor modeling; gas purification; activated carbonate–bicarbonate solution

1. Introduction

The gas purification is the term used to describe the separation of acid gas contaminants (CO_2, H_2S, SO_2, HCl, HF), organic sulfur compounds, and certain other contaminants (NH_3, NO_x, hydrocarbons, etc.) from exiting gases [1–3]. The diffuse sources are difficult to be captured and treated, and this is the reason for which the present study deals with point sources: tail gases, stacks, digesters, thermoelectric power plants, etc.

There are several main categories of the gas treating processes [2,4–7]: physical absorption, absorption with chemical reaction (chemical absorption), membrane separation, adsorption onto different solids (zeolites, activated carbon, etc.), cryogenic separation, etc. From these, the chemical absorption into liquids is a common process used for removal of acid compounds from the waste gases [8–13]. The chemical absorption processes are carried out in a variety of reactors: bubbling

absorber, packed tower, spray tower, Venturi scrubber, falling film contactor/wetted wall contactor, etc. [14].

Emissions of carbon dioxide (CO_2) into the atmosphere exhibit a major environmental problem contributing to global climate change such as global warming up, sea level change, and extreme weather conditions [15,16]. The CO_2 level in the atmosphere has almost doubled in the last period (Environmental Protection Agency (EPA)—Climate Change Indicators). Therefore, reducing the CO_2 emission is a crucial issue [15,17–19]. Regarding the technological methods which can be used for CO_2 removal, the absorption is very competitive. For enhancement of the absorption process of the carbon dioxide, potassium carbonate–bicarbonate activated solutions remain a viable method, due to recent development of new activators and high-performance charges [20–22]. Generally, chemical absorption is widely used for the elimination of the acidic gaseous components present in high concentrations in tail gases. A significant decrease of over 99% can be achieved in this way during tail gas treatment [23].

Potassium carbonate solution is an adequate solvent for carbon dioxide capture since it is cheap, environmentally friendly, resistant to degradation and evaporation, and requires low regeneration energy [23,24]. However, potassium carbonate solvent exhibits slow absorption kinetics, hence adding rate promoters such as amino acids and carbonic anhydrase, which show good reaction selectivity and fast kinetics, is necessary for improving the reaction kinetics [25–28]. By the nature of the activators, several processes are used: Giammarco–Vetrocoke (activator—arsenic trioxide; inhibitor—arsenic pentoxide), Benfield (activator—diethanolamine DEA; inhibitor—V_2O_5 or potassium metavanadate), Catacarb (activator—amine borates, inhibitor—potassium bichromate), Carsol, Carbosolvan, etc. [20,21,29,30].

In this context a mathematical model is proposed for the CO_2 absorption reactor, which was validated and proved on industrial scale. The mathematical model can be used for the CO_2 absorption from other gaseous streams such as limestone decomposition, cement installations, ceramic blocks, incinerators, etc.

The literature shows insufficient data on the mathematical modeling of the packed bed reactors when in addition to the physical absorption the chemical reaction plays also an important role [30–32]. In this context, the present study proposes and validates a mathematical model for CO_2 absorption by using hot K_2CO_3 solutions with the following composition: 25–28% K_2CO_3, 4–7% $KHCO_3$, 1.9% DEA, and 0.4% V_2O_5. The proposed mathematical model was validated by comparing the calculated values (obtained from the model) with the average values experimentally measured for a reactor used in synthesis gas manufacturing. The errors, introduced by model simplification, have been also calculated. The proposed and validated model can be used for the mathematical modeling of packed bed reactors with maximum error up to 4%. The CO_2 content of the treated gas is up to 0.2%. At the same time, the absorbed CO_2 can be easily desorbed with highly purity and can be used for carbonation processes in urea manufacture, soda ash calcination, etc.

2. Materials and Methods

The values used for model validation were obtained from industrial packed reactor. The reactor based on CO_2 absorption in activated K_2CO_3-$KHCO_3$ solutions (Chimcomplex Chemical Company, Borzești, Romania) consists of two parts of different diameters. The first part is provided with four layers of packing materials with height of 19 m and cross section area of 10.75 m^2. The second part of the reactor, with a height of 14 m of packing material placed in three layers, has a cross section area of 4.52 m^2. The packing material consists of Pall type metal rings with a nominal diameter of 50 mm. The pressure of the gas stream entering into the reactor was measured by a pressure transducer (Alicat Scientific, PC-30PSIA-D/5P, Tucson, AZ, USA). The temperature inside the reactor was measured by a thermocouple (Omega, Type K, model KMQSS-125-G-6, Norwalk, CT, USA). The pressure and temperature values were monitored and recorded. The gas concentration was determined with Online Infrared Flue Gas Analyzer-Gasboard 3000 (Wuhan, China) and liquid phases were analyzed by

titrimetric methods. The picture of the industrial plant is presented in Figure 1a. The flow fluxes given in Table 1 are presented in Figure 1b.

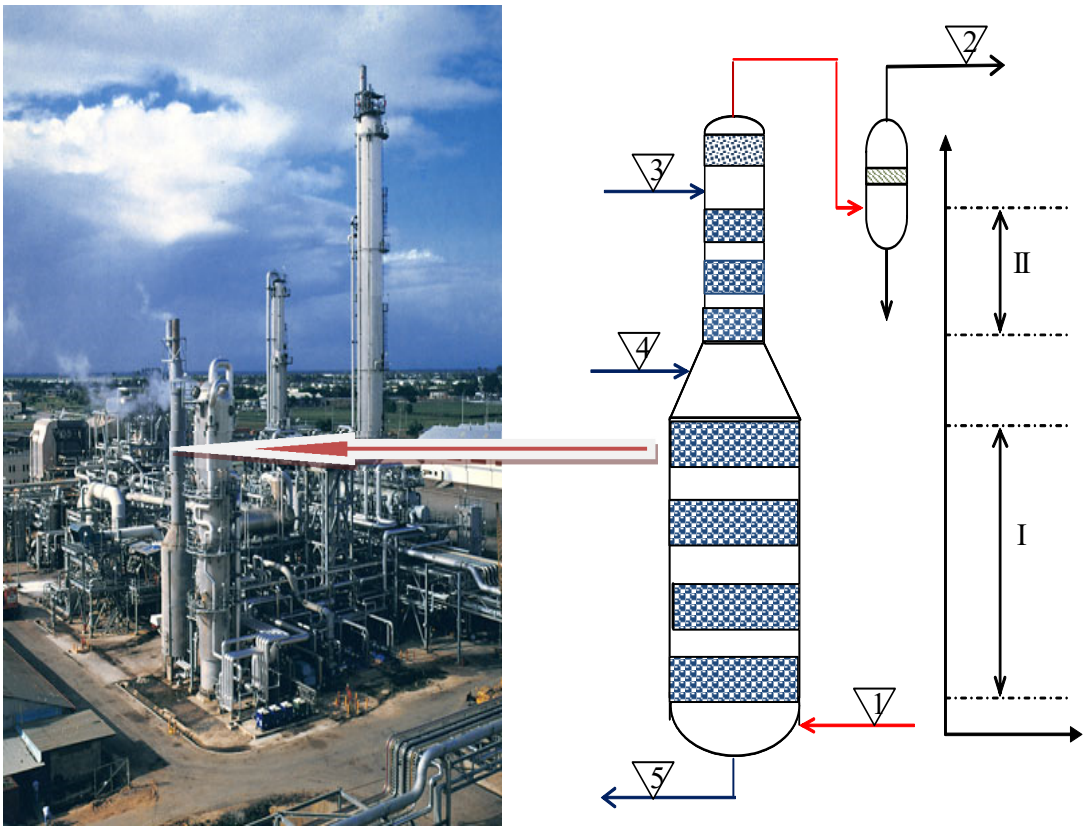

(**a**) (**b**)

Figure 1. (**a**) Industrial plant for CO_2 absorption using Carsol solution, (**b**) including the packed absorption column (industrial reactor) considered for validation of the proposed model.

Table 1. Values used in mathematical modeling of the packed bed reactor.

Values	Part I	Part II
Inlet gas temperature, K (1)	355	–
Outlet gas temperature K (2)	–	359
Inlet liquid temperature, K (3)	378	345
Outlet liquid temperature, K (5)	400	–
Pressure, atm	27	27
Gas flow, kg/h	95,657.00	45,877.00
Inlet liquid flow, kg/h	1,218,506	307,994
Column diameter, m	3.70	2.4
% CO_2 in gas (1)	21.42	–
% CO_2 in gas (2)	–	0.13
% H_2O in gas (1)	2.27	–
C_{Cb}, mol/L (3)	–	2.2878
C_{Bc}, mol/L (3)	–	1.503
C_{Cb}, mol/L (4)	1.7156	–
C_{Bc}, mol/L (4)	3.438	–
C_{Cb}, mol/L (5)	1.1091	–
C_{Bc}, mol/L (5)	4.61	–
C_{Am}, mol/L	0.01818	0.01818
n_L, kmol/s	15.89	3.099
n_g, kmol/s	1.750	–

The mathematical model of the packed bed reactor was tested by comparison of the values obtained from solving the mathematical model with the experimental values obtained from industrial scale runs. The data used for comparison were the arithmetic mean of the values experimentally determined during the 30-day operation. For validation, the values given in Table 1 have been considered. The material flows with indicators from 1 to 5 are presented in Figure 1b and the indicators are presented in Table 1 as well for easier understanding. The values summarized in Table 1 represent the mean values of 10 samples taken hourly, during 24 h, over the 30-day period.

3. Mathematical Modeling of the Packed Reactor

The setting up of the mathematical model of the packed bed reactor involves the following [23,33,34]:

expression of chemisorption rate;
characterization of phases circulation regime;
characterization of thermal regime.

The chemical process occurring in the reactor is the result of the interaction between the mass transfer of reactants from the bulk phase into the interfacial layer, as well as that of the reaction products from the interfacial layer. Contacting the gas and the liquid phases in the presence of packed material, although it is simple from reactor design point of view and advantageous from economic point of view, leads to complicated flow regimes. Therefore, simplified flow patterns are required for the further calculations. In this context, the ideal plug flow model (D) is used for the gas phase, while ideal plug flow model (D) or ideal completely-mixed flow (R), axial or radial dispersion real models, and cellular model have been used for the liquid phase [14]. The mathematical model has been devised for two cases: isothermal and adiabatic thermal regimes.

The mathematical model of the packed bed reactor is elaborated considering the following simplifying assumptions:

- stationary operating regime;
- ideal plug flow phase in the reactor;
- isothermal regime;
- isobar conditions;
- the gas phase contains one component soluble in the liquid phase (CO_2).
- K_2CO_3 reacts with the soluble gas component;
- K_2CO_3 component does not undergo transformations at the reaction temperature;
- the solvent evaporates in the first part, while condensation occurs in the second part of the reactor;
- the reaction is irreversible;
- specific heat is considered to be constant.

Since ideal plug flow pattern is assumed for both phases, the equations of the mathematical model are derived from the mass, heat, and impulse balance equations, respectively, written for an infinitesimal element of the reactor. A section element is shown in Figure 2.

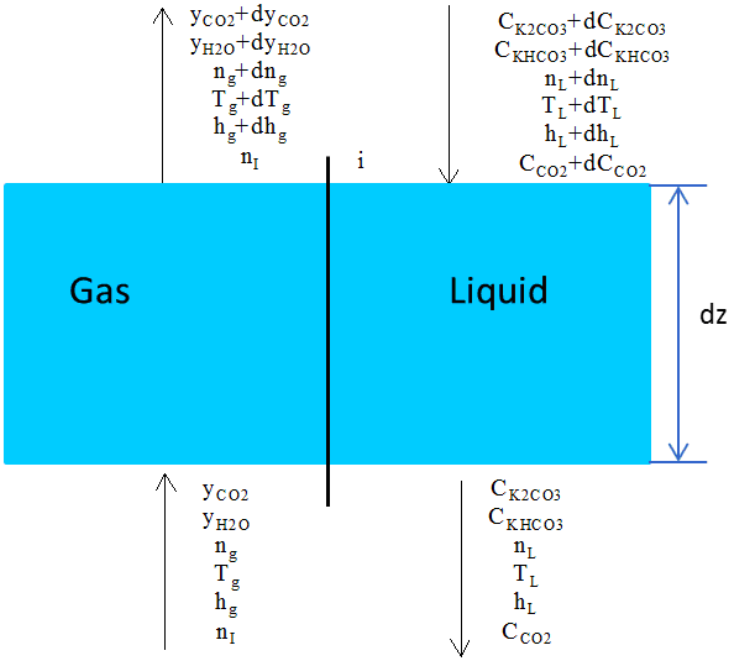

Figure 2. Differential reactor element.

For the differential reactor element as shown in Figure 2, the mass and heat balance equations were elaborated [35–39].

3.1. Mass Balance

(a) Total Mass Balance

For counter flow and stationary regime the following equations may be written:
Inlets (I):

$$\mathrm{I} = \mathrm{n_g M_g} + (n_L + dn_L)\cdot M_L \tag{1}$$

Outlets(O):

$$\mathrm{O} = (\mathrm{n_g} + dn_g)\cdot \mathrm{M_g} + n_L \cdot M_L \tag{2}$$

resulting in

$$\mathrm{n_g \cdot M_g} = \mathrm{dn_L} \cdot M_L \tag{3}$$

Equation (3) divided by dz becomes

$$\frac{\mathrm{dn_L}}{dz} = \frac{\mathrm{M_g}}{\mathrm{M_L}}\left(\frac{\mathrm{dn_g}}{\mathrm{dz}}\right) \tag{4}$$

The gas flow has been expressed considering the inert gas flow, $n_{A''}$, as

$$\mathrm{n_g} = \mathrm{n_{A''}}\left(1 + y_{CO_2} + y_{H_2O}\right) \tag{5}$$

hence

$$\mathrm{dn_g} = \mathrm{n_{A''}}\left(dy_{CO_2} + dy_{H_2O}\right) \tag{6}$$

Equation (5) divided by dz becomes

$$\frac{\mathrm{dn_g}}{dz} = \mathrm{n}_{A''}\left(\frac{dy_{CO_2}}{dz} + \frac{dy_{H_2O}}{dz}\right) \tag{7}$$

(b) Partial Molar Balance for CO_2, in Gas Phase

Inlets:

$$\mathrm{n_{A''}} \cdot y_{CO_2} \tag{8}$$

Outlets:

$$\mathrm{n_{A''}} \left(y_{CO_2} + dy_{CO_2}\right) + \nu_{CO_2} A \cdot dz \tag{9}$$

Results:

$$-\mathrm{n_{A''}}\, dy_{CO_2} = \nu_{CO_2} A \cdot dz \tag{10}$$

Equation (10) leads to

$$\frac{\mathrm{d}\dot{\mathrm{y}}_{\mathrm{CO_2}}}{\mathrm{dz}} = -\frac{1}{\dot{\mathrm{n}}_{A''}} \nu_{CO_2} A \tag{11}$$

(c) Partial molar balance for K_2CO_3, in liquid phase:

Inlets:

$$(\mathrm{n_L} + dn_L) \cdot (\mathrm{C_{Cb}} + dC_{Cb})\, \mathrm{M_L}/\rho_L \tag{12}$$

Outlets:

$$(\mathrm{n_L} \cdot C_{Cb}) \cdot\, \mathrm{M_L}/\rho_L + \nu_{CO_2} A dz \tag{13}$$

Equation (13) leads to

$$\frac{dC_{Cb}}{dz} = \frac{\rho_L}{M_L \dot{n_L}} \left(-\frac{M_L}{\rho_L} C_{Cb} \frac{d\dot{n}_L}{dz} + \nu_{CO_2} A \cdot dz \right) \tag{14}$$

(d) Partial molar balance for $KHCO_3$, in liquid phase:

Inlets:

$$(\mathrm{n_L} + dn_L)(\mathrm{C_{Bc}} + dC_{Bc})\, \mathrm{M_L}/\rho_L + 2\nu_{CO_2} A \cdot S_v dz \tag{15}$$

Outlets:

$$(\mathrm{n_L} \cdot \mathrm{C_{Bc}})\, \mathrm{M_L}/\rho_L \tag{16}$$

These result in

$$\frac{\mathrm{d}\dot{\mathrm{C}}_{\mathrm{Bc}}}{\mathrm{dz}} = -\frac{\rho_{\mathrm{L}}}{\mathrm{M_L}\dot{\mathrm{n}}_L} \left(-\frac{M_L}{\rho_L} C_{Bc} \frac{d\dot{\mathrm{n}}_L}{dz} + 2 \cdot \nu_{CO_2} A \cdot S_v \right) \tag{17}$$

(e) Partial molar balance for H_2O, in gas phase:

Inlets:

$$\mathrm{n_{A''}} \cdot y_{H_2O} \tag{18}$$

Outlets:

$$\mathrm{n_{A''}} \cdot \left(y_{H_2O} + dy_{H_2O}\right) \pm N_{H_2O} A \cdot dz \tag{19}$$

(−) for evaporation and (+) for condensation.

The mathematical model of the packed bed reactor consists of Equations (20)–(25)

$$\frac{\mathrm{dy_{CO_2}}}{\mathrm{dz}} = -\frac{1}{\dot{n_{A''}}} v_{CO_2} \cdot A \cdot S_v \tag{20}$$

$$\frac{\mathrm{dy_{H_2O}}}{\mathrm{dz}} = -\frac{1}{\dot{n_{A''}}} \left(\pm N_{H_2O}\right) \cdot A \cdot S_v \tag{21}$$

$$\frac{\mathrm{dn_g}}{\mathrm{dz}} = \dot{n_{A''}}\left(\frac{dy_{CO_2}}{dz} + \frac{dy_{H_2O}}{dz}\right) \tag{22}$$

$$\frac{\mathrm{dn_L}}{\mathrm{dz}} = \frac{M_L}{M_g}\left(\frac{d\dot{n_g}}{dz}\right) \tag{23}$$

$$\frac{\mathrm{dC_{Cb}}}{\mathrm{dz}} = \frac{\rho_L}{M_L \dot{n_L}}\left(-\frac{M_L}{\rho_L}C_{Cb}\frac{d\dot{n_L}}{dz} + v_{CO_2}\cdot A\cdot S_v\right) \tag{24}$$

$$\frac{\mathrm{dC_{Bc}}}{\mathrm{dz}} = \frac{\rho_L}{M_L \dot{n_L}}\left(-\frac{M_L}{\rho_L}C_{Cb}\frac{d\dot{n_L}}{dz} + 2\cdot v_{CO_2}\cdot A\cdot S_v\right) \tag{25}$$

M_L and M_g were calculated considering phases composition.

It is assumed that the water evaporates in the first part of the reactor, whereas in the second part the condensation of the water vapor occurs.

If the heat regime is not isothermal, the model is supplemented with the equations for the temperatures of the liquid and gas phases.

3.2. Heat Balance

(a) Total heat balance:

By using simplifying assumptions for stationary operation regime and adiabatic regime, the following equations may be written [33]:

Inlets:

$$\mathrm{n_{A''}}\, h_g + (h_L + dh_L)\cdot n_L + (-\Delta H_R)\cdot v_{CO_2}\cdot A\cdot S_v\cdot dz \tag{26}$$

Outlets:

$$\mathrm{n_{A''}}\left(h_g + dh_g\right) + n_L\cdot h_L \tag{27}$$

Resulting in:

$$n_L\cdot dh_L + (-\Delta H_R)\cdot v_{CO_2}\cdot A\cdot S_v\cdot dz = n_{A''}\cdot dh_g \tag{28}$$

The gas phase enthalpy takes the inert phase into account [40] (Das et al., 2017)

$$h_g = y_{A''}\cdot \mathrm{Cp_{A''}}\left(T_g - T_0\right) + y_{CO_2}\left[Cp_{CO_2}\left(T_g - T_0\right) + \lambda_{CO_2}\right] + y_{H_2O}\left[Cp_{H_2O}\left(T_g - T_0\right) + \lambda_{H_2O}\right] \tag{29}$$

The following equation can be given for the liquid phase

$$h_L = \mathrm{Cp_L}(T_L - T_0) + \Delta H_{dizCO_2} \tag{30}$$

(b) Heat balance for liquid phase:

Inlets:

$$(-\Delta H_R)\cdot v_{CO_2}\cdot A\cdot S_v\cdot dz + q_g\cdot A\cdot S_v\cdot dz + (n_{L.} + dn_L) \tag{31}$$

Outlets:

$$n_L\cdot h_L \tag{32}$$

Resulting in

$$(-\Delta H_R)\cdot v_{CO_2}\cdot A\cdot S_v\cdot dz + q_g\cdot A\cdot S_v\cdot dz = -n_L\cdot dh_L - h_L\cdot dn_L \tag{33}$$

The heat flow transferred through interface from gas phase q_g, is expressed by the equation

$$q_g = \alpha_g\left(T_g - T_i\right) = \alpha_L(T_i - T_L) = q_L \tag{34}$$

where dh_g and dh_L can be expressed by deriving the Equations (29) and (30).

Replacing $(-\Delta H_R)\cdot\nu_{CO_2}\cdot A\cdot S_v\cdot dz$ from Equation (28) into Equation (33) and then, substituting the expressions for dh_g, dh_L and q_g, the following equations for the gas phase temperature profile are obtained:

$$\frac{dT_g}{dz} = \frac{1}{\dot{n}_{A''}Cp_g}\left[-\alpha_g(T_g - T_i)\cdot A\cdot S_v - Cp_L(T_L - T_0)\frac{dn_L}{dz} - \dot{n}_{A''}\left[Cp_{CO_2}(T_g - T_0) + \lambda_{CO_2}\right]\frac{dy_{CO_2}}{dz} - \right.$$
$$\left. -\dot{n}_{A''}\left[Cp_{H_2O}(T_g - T_0) + \lambda_{H_2O}\right]\frac{dy_{H_2O}}{dz}\right] \quad (35)$$

$$\frac{dT_L}{dz} = \frac{1}{n_L Cp_L}\left[-\alpha_L(T_i - T_L)\cdot A\cdot S_v - Cp_L(T_L - T_0)\frac{dn_L}{dz} - (\Delta H_R)\cdot\upsilon_{CO_2}A\cdot S_v\right] \quad (36)$$

3.3. Impulse Balance

The impulse balance is elaborated for the reactor element presented in Figure 2.

The pressure loss was calculated by using the Bernoulli equation, written for an element height equal to dz, which leads to the formula [14,23,41,42]

$$-g\cdot dz + \frac{1}{2}d\left(w_g^2\right) - \frac{1}{\rho_g}dp - F = 0 \quad (37)$$

Since for gases, the gravitational forces can be neglected, the first term of the Equation (37) can be neglected. In case of the reactor that operates at relative high pressures, the pressure loss is lower compared to the pressure inside the reactor; hence, also the second term of Equation (37) can be neglected. In order to calculate F, Fanning expression was considered, where the friction factor f, depends on the packing material [35].

$$F = f\frac{dz}{d}\frac{w_g^2}{2} \quad (38)$$

The pressure loss results from the equation

$$\frac{dp}{dz} = -f\frac{w_g^2}{2\cdot d}\rho_g \quad (39)$$

On the basis of the experimental studies carried out on the industrial reactor, in the case of small pressure loss, the mathematic model of the packed bed reactor consists of Equations (11) to (25). In order to verify whether the regime is isobar, the model was supplemented with Equation (39). Since a temperature increase has been experimentally observed both for the liquid and gas phases, the mathematical model of the reactor has been also supplemented with Equations (35) and (36).

On the basis of the impulse balance, in a reactor element, the following equations are proposed for the calculation of the pressure loss along the length of the reactor [35].

1. Javaronkov and Aerov equation

$$\frac{dp}{dz} = -f\frac{w_g^2}{2\cdot d_{ech}}\rho_g\cdot\varepsilon \quad (40)$$

2. Brownell equation

$$\frac{dp}{dz} = -f\cdot F_\lambda\frac{w_g^2}{2\cdot d}\rho_g \quad (41)$$

3. Ergun equation

$$\frac{dp}{dz} = -f'\cdot\frac{1-\varepsilon}{\varepsilon^3}\frac{w_g^2}{2\cdot d_{ech}}\rho_g \quad (42)$$

4. Wall Proposed the Following Relationship for the Calculating the Pressure Loss within a Packed Bed Reactor:

$$\Delta p = 83.20 \cdot \left(\frac{a \cdot G^2}{2 \cdot g} \right)^{b \cdot L} \quad (43)$$

where a = 0.00077, and b = 0.0246, for 50 mm metallic Pall rings [23,35].

4. Testing the Proposed Mathematical Model

4.1. Testing the Mathematical Model of the Reactor under Isobar–Isotherm Conditions

The mathematical model under isobar-isothermal conditions consists of Equations (11)–(25). Meshing methods will be used to numerically solve the model. The solution consists of constructing a series $(y^{<i>})_{i=0,n}$, where $y^{<i>}$ constitutes an approximation for x(h_i). The series $y^{<i>}$ indicates the value of the solution of the differential equation in the h_i point. At the certain time, $h_0 < h_1 < \ldots h_n$ is a division of the interval where the solution is searched. For the actual reactor height, the following values have been calculated: CO_2 concentration in the gas phase (y_{CO_2}), water concentration (y_{H_2O}), the number of moles of liquid (n_L) and moles gas phase (n_g). The calculated value for y_{CO_2}, y_{H_2O}, n_g, n_L, C_{Cb}, and C_{Bc} were compared with those determined experimentally at industrial facility. The equilibrium constant of the reactions, transfer coefficients and other constants are available in the literature [42], and were publish in a previous paper [23]. In Figure 3, the variation of CO_2 molar fraction (y_{CO_2}) in the first part of the reactor is presented. Molar fraction was calculated as ratio between the moles of CO_2 reported to moles of inert gas.

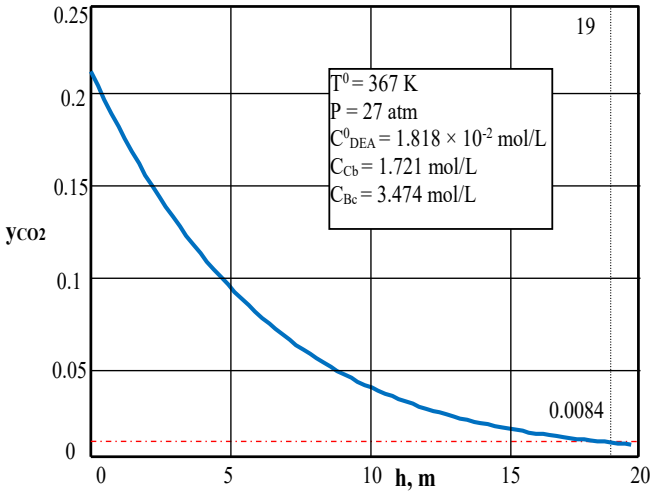

Figure 3. Variation of CO_2 molar fraction in the function of reactor height for the first part of the reactor.

A value of y_{CO_2} = 0.0084 has been obtained for the first part of the reactor. Further decrease in the CO_2 content of the gas phase can be achieved in the second part of the reactor by absorption in the regenerated solution. Considering that y_{CO_2} of 0.0084 was obtained for the first part of the reactor (19 m), it is the initial value for the gas stream entering into the second part of the reactor. The mathematical model was solved, and the profile obtained for y_{CO_2} is shown in Figure 4.

Figure 4 shows that CO_2 concentration in the gas phase leaving the second part of the reactor is equal to 0.125%. Taking into account the fact that, after solving the model, the calculated CO_2 concentration shows a 4% deviation from the concentration value measured experimentally in the industrial plant, it can be concluded that the proposed equation for the carbon dioxide molar fraction is correct.

In the first part of the reactor, where the liquid phase temperature is equal to 378 K, an increase in the water fraction in the gas phase is observed due to water evaporation. Furthermore, testing of the

proposed differential equation for the water balance of the gas phase is carried out. The y_{H_2O} fraction profile for the conditions established for the first part of the reactor is depicted in Figure 5. In the second part of the reactor, the change of the molar fraction of water, y_{H_2O}, has the profile shown in Figure 6.

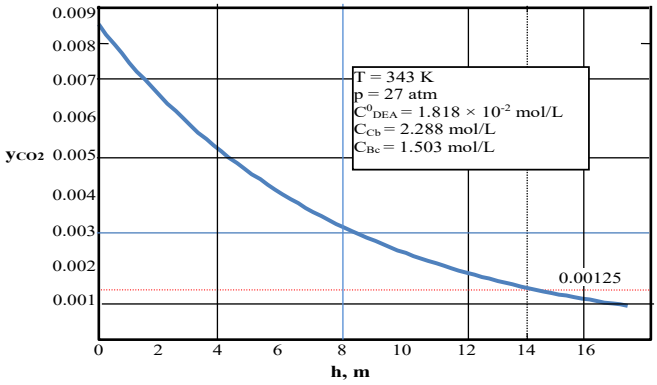

Figure 4. Variation of the y_{CO_2} with reactor height, in the second part of the reactor.

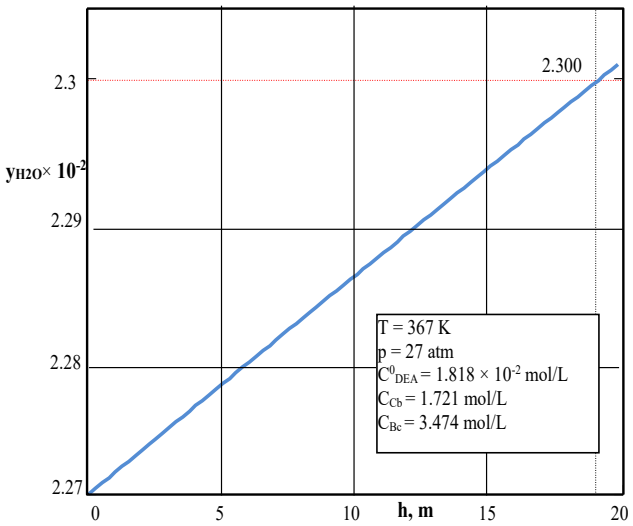

Figure 5. Variation in molar fraction of the water in the gas phase for the first part of the reactor.

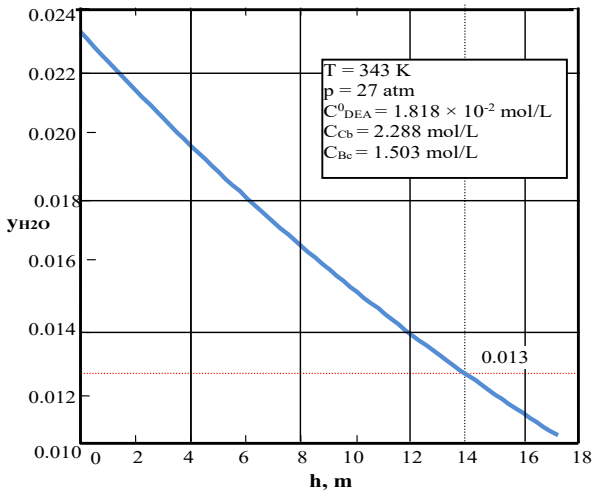

Figure 6. Variation of the water concentration in the gas phase with the reactor height for the second part of the reactor.

It is to be noted that the water content of the gas phase decreased, as a result of the fact that water vapor condensation occurred at 343 K. The value obtained by simulation is higher than the experimentally determined value. This difference is explained by the fact that the evaporation process does not take place completely in the first part of the reactor. At the bottom of the reactor, since the temperature is equal to 378 K, evaporation occurs; however, at the top of the first part of the reactor, it is possible that the water vapor condensation starts. In order to verify this assumption, it was considered that the evaporation took place at a height of 14 m of the first part. The value obtained for the water concentration was assumed to be the initial value of the condensation process. Performing the simulation for a 5 m segment of the first part and then for the second part of the reactor, value of 0.011 was obtained for the water vapors concentration. In this case, the error was 0.759%. Figure 6 reveals a decrease in the water moles due to the absorption process.

The profile obtained for the variation of gas phase moles is shown in Figure 7. In the second part of the reactor, the number of gas phase moles decreases, due to the absorption process, as well as due to the condensation of the water vapor. The number of gas phase moles obtained by simulation at the reactor outlet is 1.4748 kmol/s, as compared to the value resulting from the real mass balance, which is equal to 1.4586 kmol/s. The calculated error is equal to 1.098%.

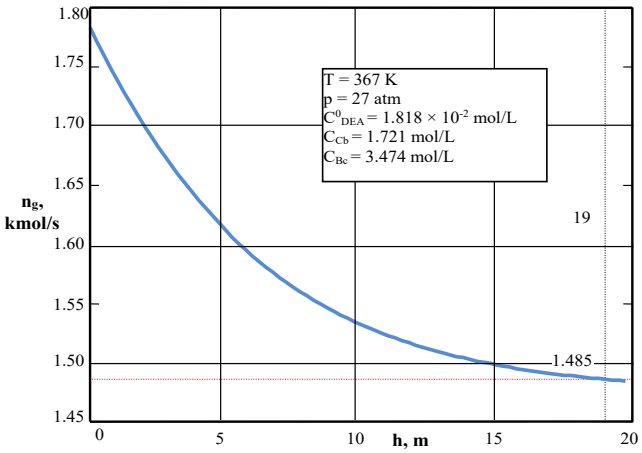

Figure 7. Variation of the total moles of gas phase with the reactor height for the first part of the reactor.

The variations in the liquid phase moles for the first and the second parts of the reactor are presented in Figures 8 and 9, respectively.

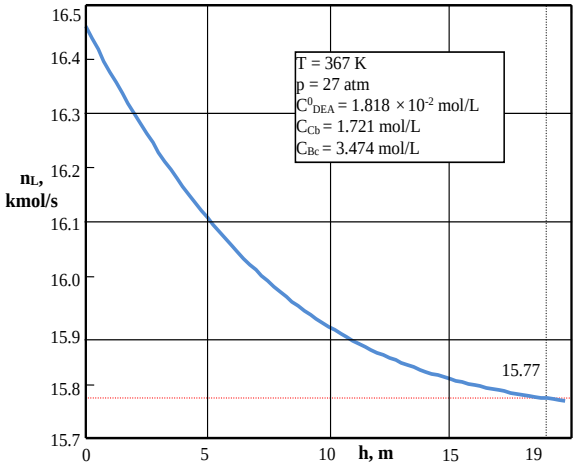

Figure 8. Variation in the liquid phase moles with the reactor height for the first part of the reactor.

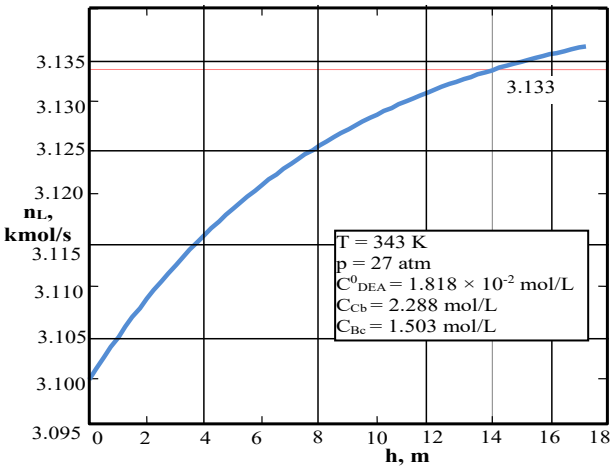

Figure 9. Variation of liquid phase moles with the reactor height for the second part of the reactor.

Analysis of the results has shown that the total moles decrease in the first part of the reactor as a result of partial evaporation of the water. The absorbed CO_2 does not change the total liquid phase moles according to the chemical reaction.

The initial liquid phase moles for the first part of the reactor have been calculated as the sum of the moles of partially regenerated solution and the number of moles of solution obtained by simulation under the conditions established for the second part of the reactor. The values obtained by simulation were compared with the values calculated from the mass balance, and the error was equal to 3.25%.

Regarding the variation of the solution concentration, Figure 10 shows the profile of the carbonate and potassium bicarbonate concentration along the first part of the reactor.

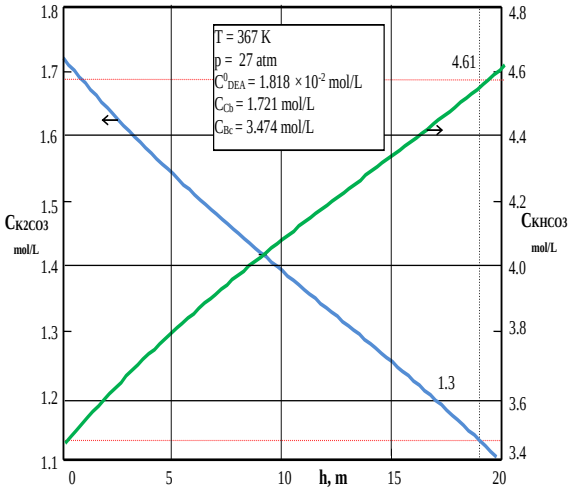

Figure 10. Profile of potassium carbonate (blue line) and bicarbonate (green line) concentrations with the reactor height for the first part of the reactor.

The concentration of potassium carbonate in the liquid phase decreases from 1.715 mol/L to 1.13 mol/L due to the chemical reaction. As an initial value, the average of the experimental values was considered. The concentration of potassium carbonate determined experimentally in the exhausted solution at the bottom of the reactor was C_{Cb} = 1.091 mol/L. The calculated error was equal to 3.39%.

The potassium bicarbonate concentration of the liquid phase, obtained by simulation, increases from 3.438 mol/L to a value of 4.61 mol/L. The composition of the outlet liquid phase was experimentally determined in order to perform the testing of the industrial reactor model. For $KHCO_3$, the error introduced by using the proposed model was equal to 0.138%.

The potassium carbonate/bicarbonate concentration profile, calculated under the conditions of the second part of the industrial reactor, is shown in Figure 11.

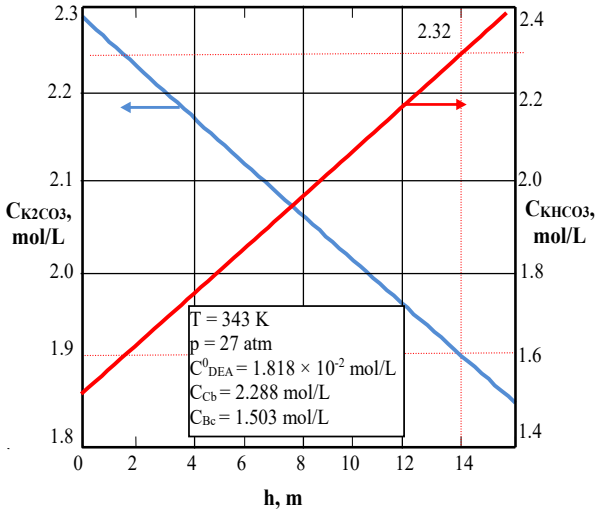

Figure 11. Variation in concentration of potassium carbonate (blue line) and bicarbonate (green line) with the reactor height for the second part of reactor.

The potassium carbonate concentration decreases from 2.3 mol/L to 1.9 mol/L (Figure 11). This value was used to calculate the mixing and to establish the initial potassium carbonate concentration in the first part of the reactor.

The value of the potassium bicarbonate concentration increases from 1.503 mol/L to 2.32 mol/L, which was further used to calculate the initial concentration of the fluid entering in the first part of the reactor.

The tests performed revealed that the proposed mathematical model for the industrial reactor using carbon dioxide absorption in diethanolamine activated potassium carbonate solutions leads to a calculation error of up to maximum 4%, in accordance with literature [43–46].

From the Equations (20)–(25), only the Equation (21) referring to the water concentration in gas phase cannot not describe perfectly the process occurring in the reactor. However, for simplicity, it was considered that water evaporates in the first part of the reactor, while in the second part, the condensation of water vapor occurs.

4.2. Testing the Mathematical Model of the Reactor under Adiabatic Conditions

Solving the mathematical model of the reactor under adiabatic conditions involves taking into account the thermal balance Equations (26)–(36), in addition to the mass balance Equations (20)–(25). The profile for the liquid phase temperature, based on the relationship (36), is presented in Figure 12.

The temperature of the liquid phase increases from 378 K for the fluid entering into the reactor to 405 K at the reactor outlet (Figure 12). This is explained by the weak exothermic effect of the process, mainly in the first part of the industrial reactor where significant part of the carbon dioxide in the gas phase enters into chemical reaction. The experimental data obtained revealed a value of 400 K for the temperature of the liquid phase which leaves the reactor. The error between the calculated and the experimentally determined value was about 1.25%.

Solving the relationship (35) leads to a gas phase temperature profile shown in Figure 13. The calculation was carried out for the conditions assumed for the first part of the reactor.

Figure 13 indicates a temperature increase from 355 K to 365 K for the gas phase. This increase is explained by the heat transfer processes that occur between the gas and the liquid phases. The temperature profile of the liquid phase under the conditions of the second reactor is shown in Figure 14. The temperature of the liquid phase in the second part of the reactor increases due to the thermal effect

of reaction at 353 K. In the second part of the reactor, the temperature increase in the liquid phase is lower due to the lower amount of carbon dioxide absorbed. In this part of the reactor a certain amount of heat comes from the latent heat of condensation of the water vapor. The temperature profile of gaseous phase in the second part of the reactor is shown in Figure 15.

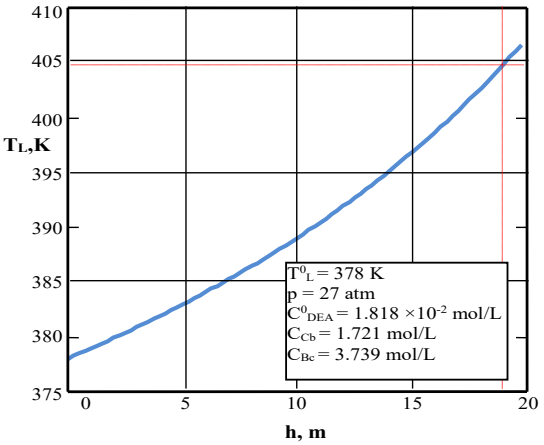

Figure 12. Variation of liquid phase temperature for the first part of the reactor.

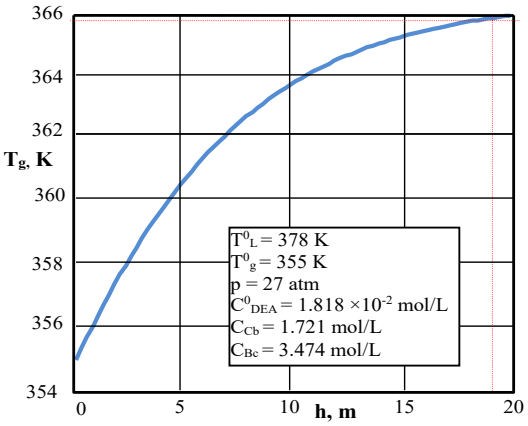

Figure 13. Profile of gas phase temperature for the first part of the reactor.

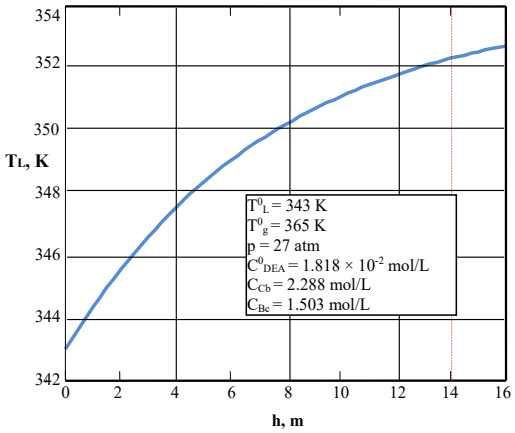

Figure 14. Variation of liquid phase temperature in the second part of the reactor.

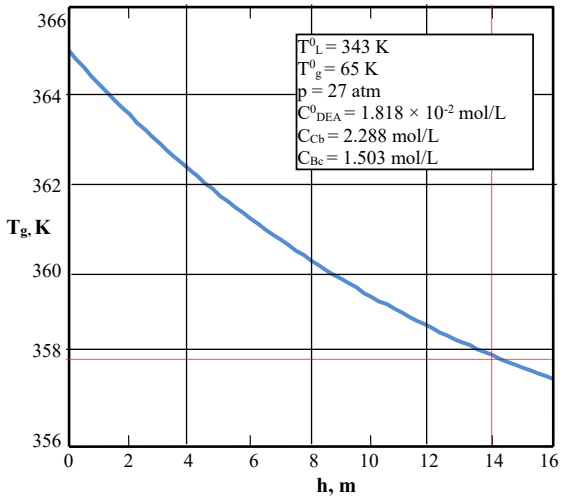

Figure 15. Variation of gas phase temperature in the second part of the reactor.

The temperature of the gas phase decreases in the second part of the reactor from 365 K to 357.5 K. This decrease is mainly due to the heat transfer from the gas phase to the liquid phase as a result of the temperature difference between the two fluids. The temperature of the gas phase measured at the reactor outlet was 359 K, the calculated error was 0.417%.

4.3. Testing the Impulse Transfer Equations

The literature provides empirical equations established on the basis of experimental determinations for the calculation of pressure loss in packed bed reactors [47,48].

Equations (41)–(43) were solved, leading to the profile of pressure loss presented in Figure 16.

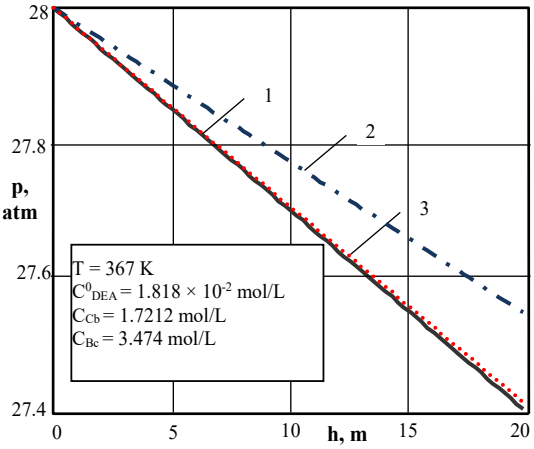

Figure 16. Pressure loss in the first part of the reactor: **1**—Equation (41), **2**—Equation (42), **3**—Equation (43).

One may see from Figure 16 that the pressure loss calculated with the aforementioned three relations have close values (around 0.55 atm at a height of the first part of 19 m). This observation demonstrates that the regime can be considered isobar. Considering the initial pressure (27.45 atm) at the inlet of the second reactor, the calculation for the second part of the reactor was performed resulting in 27.1 atm for the reactor outlet pressure. The error was equal to 3.7%.

Comparison between the experimental and calculated results is presented in Table 2.

Table 2. Values used in mathematical modeling of the packed bed reactor.

Values	Part I		Part II	
	Experimental	**Theoretic**	**Experimental**	**Theoretic**
Outlet gas temperature K	366	365	359	357.5
Outlet liquid temperature, K	400	405	345	353
Pressure, atm	28	27.45	28	27.1
% CO_2 in gas outlet	0.8077	0.84	0.13	0.125
% H_2O in gas outlet	2.27	2.30	1.31	1.30
C_{Cb}, mol/L outlet	1.1091	1.13	1.908	1.90
C_{Bc}, mol/L	4.61	4.616	2.321	2.32

The experimental values are in harmony with the results calculated on the basis of the mathematical model devised by the authors. This supports the notion that the model set up complies with the requirements and expediently can be used for industrial applications for modeling of the absorption of carbon dioxide by activated potassium carbonate solution from exit gases.

5. Conclusions

In order to test the adequacy of the mathematical model for the packed bed reactor, the differential equations have been separately solved and the values obtained by calculation were compared with those determined experimentally on an industrial scale.

At the outlet of the first part of the reactor a value for the molar concentration of carbon dioxide, y_{CO_2} = 0.0084 has been obtained, whereas at the outlet of the whole reactor a y_{CO_2} value of 0.00125 has been obtained for the gas phase. The average value of the experimental values was 0.0012. The fact that after the simulation a 4% deviation was observed between the calculated and the experimental values highlighted the fact that the proposed model was correct.

It has been found that the y_{CO_2} value increased in the first part of the reactor; suggesting that water evaporation has occurred in this section. In the second part of the reactor the fraction of water, y_{H_2O} decreased supporting the condensation of water vapor. The error calculated was 0.759%. The number of gas moles decreased due to CO_2 absorption, and also due to the process of water vapor condensation in the second part of the reactor, the error calculated was 1.098%. The calculated error for absorbent concentration is 3.39%, while for potassium bicarbonate it is only 0.138%. For temperature calculation, the input error is maximum 0.417%.

Tests carried out have demonstrated that the proposed mathematical model can be efficiently and expediently used to simulate reactor based on the carbon dioxide absorption in potassium carbonate solutions activated by diethanolamine (DEA). The maximum input error is equal to 4%, which is accepted for industrial process.

Author Contributions: Conceptualization, Methodology, Project administration, Funding acquisition, M.H.; Investigation, Visualization, G.C.; Formal analysis, Writing—original draft, T.J.; Validation, Writing—review and editing, I.C.

Acknowledgments: The authors thank to the Romanian Industrial Partner (Sofert Company, SA) for the permission to monitoring the ammonia plant, in order to validate the model for industrial reactor.

Conflicts of Interest: The authors declare no conflict of interest.

Abbreviation

A	column section, (m^2)
C_{Cb}, C_{Bc}	molar concentration of K_2CO_3 and $KHCO_3$, (mol/L)
C_{CO_2}	CO_2 concentration in the liquid phase, (mol/L)
C^0_{DEA}	molar concentration of DEA, (mol/L)
Cp_L, Cp_g	molar heat capacity at constant pressure for liquid and gas (J/mol grad)
d_{ech}	equivalent diameter, (m)
dz	elemental thickness/height of differential section element, (m)
d	diameter of the flow section, in Equations (40) and (41), (m)
f	friction factor, dimensionless
G	mass gas flow, (kg/m^2s)
g	gravitational acceleration, (m^2/s)
h	height, (m)
h_g, h_L	enthalpy of gas and liquid, (J/mol)
i	interface
L	the liquid flow, (kg/m^2s)
M_g, M_L	molar mass of gas and liquid, (g/mol)
$\dot{n}$	molar ratio
$n_{A''}$	inert gas flow, (mol/s)
n_g, n_L	molar flux of gas and liquid, (mol/s)
N_{H_2O}	molar debit of H_2O, (mol/s)
p	pressure, (atm)
S_v	gas-liquid interfacial area per unit of liquid volume (m^2/m^3)
T_g, T_L	temperature of gas and liquid, (K)
w_g	gas velocity, (m/s)
y_{CO_2}	CO_2 molar fraction
y_{H_2O}	H_2O molar fraction
z	elemental length/height of the reactor element, (m)
α_L, α_g	heat transfer coefficients for liquid and gas, (W/m^2grad)
ε	porosity
ΔH_R, ΔH_{dizCO_2}	thermal reaction effect, thermal dissolution effect, (J/mol)
λ_L, λ_g	thermal conductivity for liquid and gas, (W/m grad)
ρ_L, ρ_g	density of liquid and gas phase, (kg/m^3)
v_{CO_2}	reaction rate component CO_2 per unit of liquid volume, (mol/m^3s)
^{0}	superscript, initial

References

1. Aaron, D.; Tsouris, C. Separation of CO_2 from flue gas: A review. *Sep. Sci. Technol.* **2005**, *40*, 321–348. [CrossRef]
2. Harja, M.; Ciobanu, G.; Rusu, L.; Lazar, L. The effectiveness factor approach for chemical absorption process. *Environ. Eng. Manag. J.* **2018**, *17*, 813–820.
3. Soreanu, G.; Tomaszewicz, M.; Fernandez-Lopez, M.; Valverde, J.L.; Zuwała, J.; Sanchez-Silva, L. CO_2 gasification process performance for energetic valorization of microalgae. *Energy* **2017**, *119*, 37–43. [CrossRef]
4. Harja, M.; Rusu, L.; Barbuta, M. The viscosity and density of the aqueous solutions used for the absorption accompanied by chemical reaction. *Bull. Pol. Inst. Iasi. Chem. Chem. Eng.* **2008**, *9*, 55–62.
5. Koronaki, I.P.; Prentza, L.; Papaefthimiou, V. Modeling of CO_2 capture via chemical absorption processes —An extensive literature review. Renew. *Sustain. Energy Rev.* **2015**, *50*, 547–566. [CrossRef]
6. Isa, F.; Suleman, H.; Zabiri, H.; Maulud, A.S.; Ramasamy, M.; Tufa, L.D.; Shariff, A.M. An overview on CO_2 removal via absorption: Effect of elevated pressures in counter-current packed column. *J. Nat. Gas Sci. Eng.* **2016**, *33*, 666–677. [CrossRef]
7. Tollkötter, A.; Kockmann, N. Absorption and Chemisorption of Small Levitated Single Bubbles in Aqueous Solutions. *Processes* **2014**, *2*, 200–215. [CrossRef]

8. Omar, H.M.; Rohani, S. Removal of CO_2 from landfill gas with landfill leachate using absorption process. *Int. J. Greenh. Gas Control* **2017**, *58*, 159–168. [CrossRef]
9. Fernández, J.; Sotenko, M.; Derevschikov, V.; Lysikov, A.; Rebrov, E.V. A radiofrequency heated reactor system for post-combustion carbon capture. *Chem. Eng. Process.* **2016**, *108*, 17–26. [CrossRef]
10. Sotenko, M.; Fernández, J.; Hu, G.; Derevschikov, V.; Lysikov, A.; Parkhomchuk, E.; Rebrov, E.V. Performance of novel CaO-based sorbents in high temperature CO_2 capture under RF heating. *Chem. Eng. Process.* **2017**, *122*, 487–492. [CrossRef]
11. Onda, K.; Sada, E.; Takeuchi, H. Gas absorption with chemical reaction in packed columns. *J. Chem. Eng. Jpn.* **1968**, *1*, 62–66. [CrossRef]
12. Tait, P.; Buschle, B.; Milkowski, K.; Akram, M.; Pourkashanian, M.; Lucquiaud, M. Flexible operation of post-combustion CO_2 capture at pilot scale with demonstration of capture-efficiency control using online solvent measurements. *Int. J. Greenh. Gas Control* **2018**, *71*, 253–277. [CrossRef]
13. Tan, L.S.; Shariff, A.M.; Lau, K.K.; Bustam, M.A. Factors affecting CO_2 absorption efficiency in packed column: A review. *J. Ind. Eng. Chem.* **2012**, *18*, 1874–1883. [CrossRef]
14. Petrescu, S.; Harja, M. *Chemical Reactor for Heterogen Systems*; Venus Publishing House: Iasi, Romania, 2006.
15. Binczak, G.; Pohorecki, R.; Moniuk, W.; Jakubowska-Mordecka, Z. Studies on carbon dioxide absorption rate into solutions of K_2CO_3/$KHCO_3$ activated with amines. Industrial application of research results. *Przem. Chem.* **2017**, *96*, 681–684.
16. Wu, Y.; Mirza, N.R.; Hu, G.; Smith, K.H.; Stevens, G.W.; Mumford, K.A. Precipitating characteristics of potassium bicarbonate using concentrated potassium carbonate solvent for carbon dioxide capture. Part I: Nucleation. *Ind. Eng. Chem. Res.* **2017**, *56*, 6764–6774. [CrossRef]
17. Petrescu, S.; Mămăligă, I.; Ivaniciuc, M. Enhancement factor of the mass transfer for chemisorption process. *Rev. Chim.* **1998**, *1*, 64–67.
18. Wang, F.; Zhao, X.; Liang, Y.; Li, X.; Chen, Y. Calculation Model and Rapid Estimation Method for Coal Seam Gas Content. *Processes* **2018**, *6*, 223. [CrossRef]
19. Wang, F.; Liu, Y.; Hu, C.; Wang, Y.; Shen, A.; Liang, S. Experimental Study on Feasibility of Enhanced Gas Recovery through CO_2 Flooding in Tight Sandstone Gas Reservoirs. *Processes* **2018**, *6*, 224. [CrossRef]
20. Choi, J.H.; Kim, Y.E.; Nam, S.C.; Park, S.Y.; Chun, I.S.; Yoon, Y.I.; Lee, J.H. Promoter Characteristic Study on the K_2CO_3 Absorbents for CO_2 Capture: Mass Transfer According to Functional Group and Chain Length of Promoter. *Energy Procedia* **2017**, *114*, 898–905. [CrossRef]
21. Devries, N.P. CO_2 Absorption into Concentrated Carbonate Solutions with Promoters at Elevated Temperatures. Master's Thesis, University of Illinois at Urbana-Champaign, Champaign, IL, USA, 2014.
22. Khan, A.A.; Halder, G.N.; Saha, A.K. Experimental investigation on efficient carbon dioxide capture using piperazine (PZ) activated aqueous methyldiethanolamine (MDEA) solution in a packed column. *Int. J. Greenh. Gas Control* **2017**, *64*, 163–173. [CrossRef]
23. Harja, M.; Siminicanu, I. Modelling and simulation of the industrial reactor for carbon dioxideabsorption into activated potassium carbonate aqueous solution. *Ovidius Univ. Ann. Chem.* **2000**, *XI*, 135–139.
24. Cowan, R.M.; Jensen, M.D.; Pei, P.; Steadman, E.N.; Harju, J.A. *Current Status of CO_2 Capture Technology Development and Application*; National Energy Technology Laboratory, US Department of Energy: Morgantown, WV, USA, 2011.
25. Hilliard, M.D. A Predictive Thermodynamic Model for an Aqueous Blend of Potassium Carbonate, Piperazine, and Monoethanolamine for Carbon Dioxide Capture from Flue Gas. Ph.D. Thesis, University of Texas at Austin, Austin, TX, USA, 2008.
26. Sivtsova, O.N.; Eremenko, S.I.; Derevschikov, V.S.; Veselovskaya, J.V. Kinetics of carbon dioxide absorption from air in a flow reactor with a fixed bed of K_2CO_3-based sorbent. *Russ. J. Phys. Chem. A* **2017**, *91*, 850–855. [CrossRef]
27. Tay, W.H.; Lau, K.K.; Shariff, A.M. High performance promoter-free CO_2 absorption using potassium carbonate solution in an ultrasonic irradiation system. *J. CO_2 Util.* **2017**, *21*, 383–394. [CrossRef]
28. Zhang, S.; Lu, Y. Surfactants facilitating carbonic anhydrase enzyme-mediated CO_2 absorption into a carbonate solution. *Environ. Sci. Technol.* **2017**, *51*, 8537–8543. [CrossRef] [PubMed]
29. Hagiu, C.; Ivaniciuc, M. Determination of the enhancement factor for CO_2 absorption in activated potassium carbonate solution. *Rev. Chim.* **1997**, *10–11*, 856–862.

30. Hu, G.; Smith, K.; Wu, Y.; Kentish, S.; Stevens, G. Recent progress on the performance of different rate promoters in potassium carbonate solvents for CO_2 capture. *Energy Procedia* **2017**, *114*, 2279–2286. [CrossRef]
31. Bui, M.; Gunawan, I.; Verheyen, V.; Feron, P.; Meuleman, E.; Adeloju, S. Dynamic modelling and optimisation of flexible operation in post-combustion CO_2 capture plants: A review. *Comput. Chem. Eng.* **2014**, *61*, 245–265. [CrossRef]
32. Saidi, M. Mathematical modeling of CO_2 absorption into reactive DEAB solution in packed columns using surface-renewal penetration theory. *J. Taiwan Inst. Chem. E* **2017**, *80*, 301–313. [CrossRef]
33. Altway, A.; Susianto, S.; Suprapto, S.; Nurkhamidah, S.; Nisa, N.I.F.; Hardiyanto, F.; Altway, S. Modeling and Simulation of CO_2 Absorption into Promoted Aqueous Potassium Carbonate Solution in Industrial Scale Packed Column. *Bull. Chem. React. Eng. Catal.* **2015**, *10*, 111–124. [CrossRef]
34. Xu, Z.; Afacan, A.; Chuang, K. Predicting mass transfer in packed columns containing structured packings. *Chem. Eng. Res. Des.* **2000**, *78*, 91–98. [CrossRef]
35. Harja, M. Contributions to the Modeling of Gas—Liquid Absorption with Chemical Reaction. Ph.D. Thesis, "Gheorghe Asachi" Technical University of Iasi, Iasi, Romania, 1999.
36. Salvinder, K.M.S.; Zabiri, H.; Isa, F.; Taqvi, S.A.; Roslan, M.A.H.; Shariff, A.M. Dynamic modelling, simulation and basic control of CO_2 absorption based on high pressure pilot plant for natural gas treatment. *Int. J. Greenh. Gas Control* **2018**, *70*, 164–177. [CrossRef]
37. Tang, L.; Ji, J.; Cai, Y.; Qu, G. Study on Mass Transfer Rate of CO_2 Absorption Process. *Int. J. Dyn. Fluids* **2017**, *13*, 335–344.
38. Todinca, T.; Tănasie, C.; Pröll, T.; Căta, A. Absorption with chemical reaction: Evaluation of rate promoters effect on CO_2 absorption in hot potassium carbonate solutions. *Comput. Aided Chem. Eng.* **2007**, *24*, 1065–1070.
39. Wang, G.; Yuan, X.; Yu, K. Review of mass-transfer correlations for packed columns. *Ind. Eng. Chem. Res.* **2005**, *44*, 8715–8729. [CrossRef]
40. Das, B.; Deogam, B.; Mandal, B. Experimental and theoretical studies on efficient carbon dioxide capture using novel bis (3-aminopropyl) amine (APA)-activated aqueous 2-amino-2-methyl-1-propanol (AMP) solutions. *RSC Adv.* **2017**, *7*, 21518–21530. [CrossRef]
41. Aroonwilas, A.; Chakma, A.; Tontiwachwuthikul, P.; Veawab, A.; Austgen, D.M.; Rochelle, G.T.; Peng, X.; Chen, C.C. Mathematical modelling of mass transfer and hydrodynamics in CO_2 absorbers packed with structured packings. *Chem. Eng. Sci.* **2003**, *58*, 4037–4053. [CrossRef]
42. Benadda, B.; Kafoufi, K.; Monkam, P.; Otterbein, M. Hydrodynamics and mass transfer phenomena in counter-current packed column at elevated pressures. *Chem. Eng. Sci.* **2000**, *55*, 6251–6257. [CrossRef]
43. Yancheshmeh, M.S.; Radfarnia, H.R.; Iliuta, M.C. High temperature CO_2 sorbents and their application for hydrogen production by sorption enhanced steam reforming process. *Chem. Eng. J.* **2016**, *283*, 420–444. [CrossRef]
44. Palys, M.; McCormick, A.; Cussler, E.; Daoutidis, P. Modeling and optimal design of absorbent enhanced ammonia synthesis. *Processes* **2018**, *6*, 91. [CrossRef]
45. Razi, N.; Svendsen, H.F.; Bolland, O. Simulation of post-combustion CO_2 capture system using new effective interfacial area correlation. *Energy Procedia* **2014**, *51*, 169–175. [CrossRef]
46. Yasari, E. A green industrial scale di-methyl ether reactor with aiming to CO_2 reduction: Staging and multi-objective optimization approach. *J. Taiwan Inst. Chem. E* **2017**, *81*, 110–118. [CrossRef]
47. Erans, M.; Manovic, V.; Anthony, E.J. Calcium looping sorbents for CO_2 capture. *Appl. Energy* **2016**, *180*, 722–742. [CrossRef]
48. Diego, M.E.; Arias, B.; Méndez, A.; Lorenzo, M.; Díaz, L.; Sánchez-Biezma, A.; Abanades, J.C. Experimental testing of a sorbent reactivation process in La Pereda 1.7 MWth calcium looping pilot plant. *Int. J. Greenh. Gas Control* **2016**, *50*, 14–22. [CrossRef]